

Dislocation Arrangements in Deformed and  
Neutron Irradiated Zirconium and  
Zircaloy-2

R. B. Roy



AKTIEBOLAGET ATOMENERGI  
STOCKHOLM, SWEDEN 1963



DISLOCATION ARRANGEMENTS IN DEFORMED AND NEUTRON  
IRRADIATED ZIRCONIUM AND ZIRCALOY-2

Ram B. Roy

Abstract

Dislocation arrangements in deformed and neutron irradiated Zr and Zircaloy-2 have been studied by thin film transmission electron microscopy. Results indicate that the prominent slip system, in both Zr and Zircaloy-2, is the  $\{10\bar{1}0\}$   $1/3 \langle 12\bar{1}0 \rangle$  type; no evidence for basal slip was observed. Attractive and repulsive dislocation interactions seem to be more important than the intersection jog reactions. Elongated loops and dipoles were seen at higher deformations and it is suspected that such loops or dipoles are formed due to interactions between dislocations lying in parallel planes.

Stacking fault ribbons lying in  $\{10\bar{1}0\}$  plane have been found in 15% cold rolled Zircaloy-2; a rough estimate of stacking fault energy indicates that it is  $\sim 65$  ergs/cm<sup>2</sup>. Calculations show that the equilibrium separation of partials is  $\sim 60$  Å and a stress as high as  $19 \times 10^{-3} \mu$  acting along  $[0001]$  direction is needed to separate them. It has been suggested that O<sub>2</sub> and N<sub>2</sub> in addition to their solid solution hardening effect may also cause a lowering of the stacking fault energy and Suzuki hardening.

## LIST OF CONTENTS

	Page
1. Introduction	3
2. Dislocation arrangement in cold rolled zirconium and Zircaloy-2	4
3. Dislocation arrangements in neutron irradiated zirconium foils	10
References	13
Appendix	15

## 1. Introduction

1.1 The dislocation arrangement in Zr has been studied previously both in unirradiated and irradiated conditions. Bailey (1) has found that the dislocation arrangement in deformed ( $\sim 1$  % in tension) Zr depends upon the purity of the material. In commercial Zr the dislocations are untangled and tend to remain confined to  $\{10\bar{1}0\} < \bar{1}2\bar{1}0 >$  slip systems, whereas dislocations in crystal bar Zr show tangling tendencies. Bailey assumed the possibility of some basal slip to account for tangling. From his results he concludes that the efficiency of  $O_2$ , C, and  $N_2$  in increasing the hardenability of Zr lies in the fact that the above impurities not only raise the stress for continued slip on the prismatic planes but also increase the stress for basal slip to prohibitively high values.

Rappoport (2) and Rappoport & Hartley (3) have determined the slip system in commercial Zr and found no evidence of slip other than  $\{10\bar{1}0\} < \bar{1}2\bar{1}0 >$  at temperatures up to  $1073^\circ K$ . Williams et al. (4), however, have postulated that some basal slip is necessary to account for the observed texture in cold rolled Zr. Howe (5) has studied the effect of irradiation on the dislocation arrangement in annealed and cold worked Zr foils. His investigations included irradiation with neutrons,  $\alpha$  particles and deuterons at various temperatures. In no case was any effect of irradiation on the dislocation arrangement detected.

With the above in mind it was decided to examine the mode of deformation and dislocation arrangements in deformed and irradiated Zr in more detail. To this end Zr foils were deformed by cold rolling to 5 to 15 % reduction in thicknesses and the change in dislocation arrangement and slip systems, dislocation reactions, production of faults etc as a function of deformation were systematically followed. The results presented here are incomplete but interesting enough to be reported. More detailed results are at present being obtained. In addition to working with commercially pure zirconium a parallel experiment with Zircaloy-2 was also made. As yet

results are not available for crystal bar zirconium but these will be forthcoming shortly.

1.2 Experimental techniques were the same as used in a previous study and are described in an earlier report (6). It is convenient to report the present work in two parts, namely

- i) Dislocation arrangement in cold rolled zirconium and Zircaloy-2
- ii) Dislocation arrangement in neutron irradiated zirconium foils.

## 2. Dislocation arrangement in cold rolled zirconium and Zircaloy-2

2.1 A qualitative comparison of dislocations in zirconium and Zircaloy-2 may be made with the help of figs. 1a to 4b. It is seen that they fall into four distinct classes and each class in Zr has its counterpart in Zircaloy-2. It is not fully clear how these distributions are formed but it is suspected that several mechanisms are involved as described in the following sections.

2.2 The types of dislocation shown in figs. 1a to 2b are typical of both small and large deformations except in that at large deformations short dislocations (figs. 2a, 2b) are overwhelmingly predominant. A preponderance of short dislocations over long ones may arise in various ways e.g.

- a) Pronounced texture in the foil
- b) Expanding loops with their ends anchored at a surface
- and c) With an increasing density of dislocations in the glide plane, the screw component of the dislocation ring can climb, leaving the predominantly edge section in the original plane.

All of the above three mechanisms may operate simultaneously but with increasing deformation, mechanism c) will perhaps become increasingly important.

For all the orientations analysed these dislocations lie in  $\{10\bar{1}0\}$  plane, the short dislocations being predominantly edge in character (see fig. 11). This supports the view that mechanism c) is responsible for the large population of predominantly edge dislocation segments at higher deformations. The Burgers vectors  $\vec{b}$  of these dislocations were assumed to be of the  $1/3 \langle \bar{1}2\bar{1}0 \rangle$  type. However, in a more detailed experiment  $\vec{b}$  will be established by tilting and heating foils in the microscope. Pile-ups (6, 1) so frequently seen both in Zr and Zircaloy are perhaps due to these short segments of edge dislocations. Fig. 6 shows some complex reactions of short dislocations with a long dislocation and also among themselves.

Another feature of dislocation arrangement which was characteristic of heavily worked material (i. e. 10 % or more) is shown in figs. 4a-b. These dislocation segments are in general paired and sometimes, especially in Zr, appear as bands of elongated loops. For the orientations analysed, they lie in  $\{10\bar{1}0\} \langle \bar{1}2\bar{1}0 \rangle$  system, figs. 7 & 8. Fig. 4a shows the band at higher magnifications. These elongated loops may be edge dipoles. The mechanism of dipole formation has been treated by Gillman (7), Tetelman (8) and Washburn (9). Elongated loops (or dipoles) provide extra barriers to dislocation movement and cause work hardening (note the jogged nature of B family of dislocations in fig. 4a, see fig. 9 for dipoles).

The dislocation arrangements illustrated by figs. 3a & 3b were quite often seen in heavily cold worked Zr and Zircaloy foils. A diffraction pattern for Zr is not available but in the case of Zircaloy, fig. 10, the intersecting pairs of dislocations seem to lie in  $\{10\bar{1}0\}$  and  $\{01\bar{1}2\}$  planes;  $\{01\bar{1}2\}$  is not an observed slip plane but it is conceivable that under the conditions of rolling some slip may occur on  $\{01\bar{1}2\}$  planes. This, however, has to be checked by more careful experiments.

2.3

In all the foils containing 5 to 10 % cold work, stacking

faults were never observed (though they might have remained undetected). However, 15 % cold worked Zircaloy readily showed areas containing stacking faults if the specimen was thin enough, fig. 13. A selected area diffraction pattern showed that the faults lie in the  $\{10\bar{1}0\}$  plane. If this analysis is correct then the fault can arise only through the following type of dissociation:

$$1/3 [\bar{1}2\bar{1}0] = 1/6 [\bar{1}2\bar{1}1] + 1/6 [\bar{1}2\bar{1}\bar{1}]$$

The stacking fault ribbons were quite long and were observed only in very thin areas. One cannot estimate accurately the stacking fault energy from widely separated partials because of their metastable nature; however, a rough calculation shows that the fault energy in Zircaloy-2 is of the order  $65 \text{ ergs/cm}^2$  \* but this estimate may well be in error by a factor of 2. Assuming that  $\gamma = 65 \text{ ergs/cm}^2$  in Zircaloy, the equilibrium separation of partials in prismatic planes is about  $60 \text{ \AA}$ , which at 20,000 magnification will be barely discernable (0.12 mm or less depending upon the orientation). The force needed to separate these partials is estimated to be  $\sim 19 \times 10^{-3} \mu$  ( $\mu$  = shear modulus) which is quite high. This perhaps explains why stacking faults were not observed at lower degrees of cold work.

It is reasonable to assume that the stacking fault energy in Zr will be somewhat higher and hence separation of partials will need even higher stresses and hence higher degree of cold work before they are formed.

2.4 The main characteristics of dislocation arrangement in 5-15 % cold worked Zr and Zircaloy-2 can be said to be

- a) Absence of tangling up to 15 % cold work
- b) Absence of cross slipping under ordinary beam heating
- c) Abundance of pile-ups

-----

\* See appendix for detail.

- d) Appearance of cusps, see fig. 12
- e) Dislocation reactions producing paired dislocations (or elongated loops) etc.

We shall discuss each of them briefly.

The observations a), b) and c) are connected in as much as what is responsible for pile-ups is also responsible for the absence of tangling. The basic mechanisms for tangling have been proposed to be:

- a) dislocation intersection jogs
  - b) cross slip
- and c) interaction between point defects and dislocations (10).

Intersection jogs are not important in case of Zr because of the kind of dislocation interactions in Zr (this, however, will be considered in more detail in the next section). Cross slip is a thermally activated process and the experimental results indicate that cross slip in Zr is rather difficult under ordinary conditions. This could perhaps be due to the dissociation of full dislocations into partials. The view that interactions between dislocations and point defects (10) are the real cause of tangling has been criticised. However, Mader (11) has shown that this mechanism could be responsible for tangling in metals of high stacking fault energy such as Al, but not in cases where the stacking fault energy is relatively low. In the latter class of material the level of stacking fault energy controls the dislocation arrangement. In view of the above facts, it is believed that the absence of tangling in Zr and Zircaloy-2 is due to the paucity of intersection jog reactions and the relatively low stacking fault energy. Wilsdorf & Wilsdorf (10) have examined the effect of dislocation arrangement during specimen preparation and came to the conclusion that tangling is not caused by such arrangement.

The only way intersection jog interaction may occur in Zr is by the dislocations threading the prismatic planes at right angles. These dislocations will lie in basal planes and will have to be predominantly edge in character. Statistically such dislocations

will be only half of the total dislocation population in basal planes and the density of dislocation in basal planes will not increase with the progress of deformation; thus it seems clear that jog formation will occur only to a very limited extent. However, these jogs can give rise to cusps on a screw dislocation, fig. 9, and formation of dipoles fig. 12, to a certain extent. In view of the fact that paired dislocations or dipoles are seen quite frequently, it appears reasonable to assume that Tetelman's (8) mechanism of dipole formation may be more important in Zr. In this mechanism dipoles are formed due to interaction of dislocations in parallel slip planes.

Saada (12) has considered the dislocation interactions in detail and Friedel (13) and Seeger et al. (14) have incorporated his results in their model of work hardening in metals. In Saada's treatment a dislocation tree (immobile dislocation) can repel or attract the moving dislocation depending on their mutual orientation and their Burgers vectors; thus when two dislocations come into contact, they interact with one another. The kind of interaction depends upon the following considerations, namely:

- 1) If the scalar product of the Burgers vectors of the meeting dislocations is negative, the interaction is attractive and junction reaction will be favored. The stress required to push the mobile dislocations through such forests is independent of temperature.
- 2) If the scalar product of the Burgers vectors of meeting dislocations are positive, the repulsive reaction is more favorable. The stress necessary to free the moving dislocation is smaller relative to the attractive case and is temperature dependent.
- 3) When the Burgers vectors of the moving dislocations are parallel and they meet at  $90^\circ$ , jog formation is the favored interaction and the stress necessary to

push the mobile dislocation past such obstacles is weak and temperature dependent.

The flow stress of a metal in general has two components

- a) temperature independent component
  - i) the stress, in addition to other sources of lattice friction, to move a dislocation due to long range stresses caused by pile-ups and dislocation lying in parallel planes -  $\sigma_L$
  - ii) the stress necessary to move a dislocation through obstacles due to junction reaction -  $\sigma_A$
- b) temperature dependent component
  - i) the stress necessary to form and move jogs -  $\sigma_j$
  - ii) the stress necessary to move dislocations through obstacles due to repulsive interactions -  $\sigma_R$ .

In general  $\sigma_A$  is quite large compared with  $\sigma_R$  and  $\sigma_j$ .

The observed slip system in Zr is the  $\{10\bar{1}0\} 1/3 \langle \bar{1}2\bar{1}0 \rangle$  type. Then, on the basis of arguments 1, 2 and 3 above, it seems that intersection interactions of dislocations in Zr will be mostly of the attractive and repulsive types. If this is the case, the flow stress in pure Zr should be less temperature dependent than in Mg and Zn, where jog formations is also important due to the occurrence of basal glide. Reliable data on the flow stress is not available but experiments to determine this are planned.

2.5 Churchman (15) has stipulated that the hardness value of Zr is so sensitive to its  $O_2$  and  $N_2$  content that it can be taken as a measure of its  $O_2$  and  $N_2$  content. Bailey (1), on the basis of his electron microscope studies of the dislocation arrangement in commercial and crystal bar Zr, has come to the conclusion that  $O_2$  and  $N_2$  somehow or other restrict cross slip and keep the dislocations confined to their glide planes (i. e. prismatic plane). This is rather surprising because  $O_2$  and  $N_2$  should make the basal

slip more favorable (and hence even cross slip) by increasing the  $c/a$  ratio.

However, if one assumes that apart from their solid solution hardening effect,  $O_2$  and  $N_2$  can also lower the stacking fault energy in Zr, then one can visualise an extra hardening effect just due to this cause. This might happen in two ways, namely

- i) lowering of stacking fault energy will cause partials to be widely separated both in prismatic and basal planes and hence prevent the dislocations from cross slipping,
- ii) migration of impurities to the faulted area may cause Suzuki hardening.

This kind of hardening, however, will be temperature dependent and add to the temperature dependent component of the flow stress.

That oxygen is capable of decreasing the stacking fault energy is supported by the fact that widely extended stacking fault ribbons have been observed in heavily oxidised Zr foils (16).

### 3. Dislocation arrangements in neutron irradiated zirconium foils

- 3.1 The mechanical properties of Zr are significantly changed by irradiation and one expects that the dislocation arrangement should be accordingly altered to account for the observed changes in yield and tensile strengths. Reported work (2) on electron microscope studies of dislocation arrangement in irradiated Zr, however, has given negative results, which is surprising; it was therefore considered worth-while to make an independent experiment in this connexion.
- 3.2 Vacuum annealed ( $735^{\circ}C$ , 12 hrs) foils of Zr (0.05 mm thick) were sealed into Al cans and irradiated in the R2 reactor. The cans were in direct contact with the primary cooling water which has

temperature  $\sim 40^{\circ}\text{C}$ . The neutron flux during irradiation was  $2 \times 10^{13} \text{ n/cm}^2/\text{sec}$ . and the total dose received  $3 \times 10^{18} \text{ nvt}$  corresponding to  $\sim 2.7 \times 10^{18} \text{ nvt} > 1 \text{ MeV}$ . The appearance of the foils gave no visible sign of oxidation or mechanical damage. Microscope specimens were prepared in the usual way (6).

- 3.3 Results are presented in figs. 15 to 22. In nearly all specimens small black dots were seen. These dots were fairly evenly distributed and varied in size from  $\sim 65$  to  $4000 \text{ \AA}$  or more. When the specimen was tilted, they gave contrast effects similar to dislocation loops, figs. 18 & 20. Furthermore, the size and shape of the dots varied during tilting, figs. 18 & 19. From what is known at the moment, these defects behave like precipitates. Hydride or oxides are the most probable possibilities but further experiments are needed to clarify the issue.
- 3.4 Compared to the dislocation population in an annealed unirradiated specimen, irradiated foils were fairly well populated with dislocations; these dislocations might, however, have been introduced during handling. Dislocations were seen to be invariably pinned by the dots described above, figs. 15 & 16. For the orientations analysed they lay in  $\{10\bar{1}0\}$  plane, fig. 15. Many dislocations were bowed out between the pinned points. Diffraction pattern analysis is not available at the moment but a rough estimate shows that a stress as high as  $7 \times 10^{-4} \mu$ , where  $\mu$  is the shear modulus, is acting on some of the bowed dislocations. Interesting dislocation reactions and pile-ups were observed, figs. 17 & 22.
- 3.5 The black dots behave like precipitates on tilting, part of the evidence for this lies in the fact that the line of no contrast in the loop is perpendicular to  $g$ , the latter being the reciprocal lattice vector. Unfortunately more than one strong reflection was operating and hence it is not certain which reflection was responsible for the contrast. However, it has been assumed that  $g$  perpendicular to the line of no contrast is the operating one. The dark side of the images lies on the side of positive  $g$  and the light side on the side of negative  $g$ . Thus, these precipitates cause an expansion of the

lattice (17). Both hydrides and oxides of Zr have larger lattice parameters than Zr.

3.6           The general appearance of the dislocations is appreciably different from what is seen in unirradiated specimens. They are no longer straight and form complex shapes e.g. as at A, B and C in fig. 17. At A both attractive and repulsive types of reaction can be seen. Bowing out of dislocations and the presence of pile-ups show that dislocation movement has occurred. The tail end of pile-ups at 'C' in fig. 22 seem to have cross slipped under stress. Pinning of the dislocations indicates that neutron irradiated Zr should show "yield drop" on tensile testing and this has in fact been observed in irradiated hydrogen loaded Zircaloy. Howe (2) has also reported a yield point for Zr specimens which were irradiated in pressurised water at 270°C.

References

- (1) J.A. Bailey, Electron microscope studies of dislocations in deformed zirconium. - J. Nucl. Mat. 7 (1962) p. 300
- (2) E.J. Rappoport, Room temperature deformation process in zirconium. - Acta Met. 7(1959) p. 254
- (3) E.J. Rappoport and C.S. Hartley, Deformation on modes of zirconium at 77<sup>o</sup>, 575<sup>o</sup> and 1075<sup>o</sup>K. - Trans. AIME 218(1960) p. 869
- (4) D.N. Williams and D.S. Eppelsheimer, Origin of the deformation textures of Titanium. - Nature 170(1952) p. 146
- (5) L. Howe et al., Radiation damage in zirconium, Zircaloy-2, and 410 stainless steel. - Symposium on Radiation Damage in Solids and Reactor Materials, I.A.E.A. Venice, 1962. Paper No. SM 25/13.
- (6) R.B. Roy, Dislocations in cold worked Zr and Zircaloy. 1963. (RMA-406).
- (7) W.G. Johnston and J.J. Gilman, Behaviour of individual dislocations in strained-hardened LiF crystals. - J. Appl. Phys. 31(1960) p. 687.
- (8) A.S. Tetelman, Deformation dipole formation in crystals. Acta Met. 10(1962) p. 813.
- (9) J. Washburn, Strain hardening, strengthening mechanism in solids. Publ. by The American Society for Metals, Metals Park, Ohio, 1963. p. 51
- (10) K. Wilsdorf and H.G.F. Wilsdorf, On the origin of dislocation tangles and long prismatic dislocation loops in deformed crystals.- Electron microscopy and strength of crystals. Interscience Publishers, New York, 1963, p. 575.
- (11) S. Mader, Surface and thin foil observations of the substructures in deformed FCC and HCP metal single crystals, Ibid, p. 183

- (12) G. Saada, Dislocation interactions and plastic deformation in crystals. Ibid, p. 651.
- (13) J. Friedel, On the elastic limit of crystals. Ibid, p. 605.
- (14) A. Seeger, S. Mader and H. Kronmuller, Theory of work-hardening of FCC and HCP single crystals. Ibid, p. 665.
- (15) A.T. Churchman, The slip modes of Titanium and the effect of purity on their occurrence during tensile deformation of single crystals. - Proc. Roy. Soc. A226(1954) p. 216
- (16) J.A. Bailey, On the oxidation of thin films of zirconium, Letters to the editors. - J. Nucl. Mat. 8(1963) p. 259.
- (17) M.F. Asby and L.M. Brown, Diffraction contrast from spherically symmetrical coherency strains. - Phil. Mag. 8(1963) p. 1083.

APPENDIX

Calculation of stacking fault energy

We will consider the dissociation of a pure edge in the  $(1\bar{1}00)$  plane. It is expected that the method of calculation described here will also be valid for a pure screw. The partials arise from the following dissociation, viz:

$$1/3 [11\bar{2}0] = 1/6 [11\bar{2}1] + 1/6 [11\bar{2}\bar{1}] \quad (1)$$

Writing in the notation of 3 indices<sup>\*</sup>, equation (1) becomes

$$[10\bar{1}] = 1/6 [41\bar{2}] + 1/6 [2\bar{1}\bar{4}] \quad (2)$$

Then, following the notations of fig. 1, a stress  $\tau$  acting along the  $[111]$  direction in the  $[1\bar{2}1]$  plane will have zero component along  $a_1$  and  $a_2$  but will exert an equal and opposite force on  $\beta_1$  and  $\beta_2$  and hence forcing them to separate

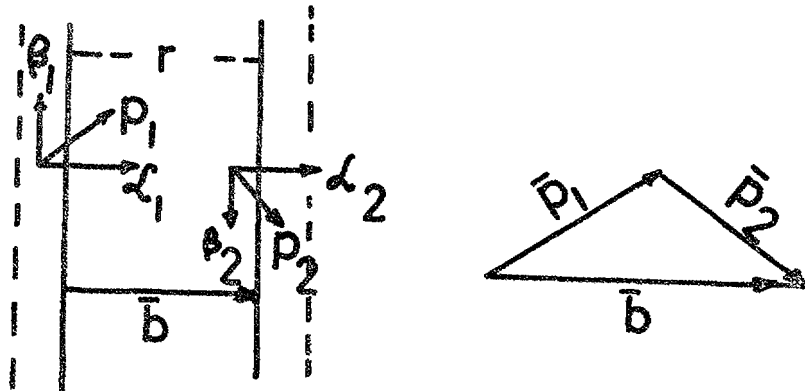


Fig. 1  $P_1$  and  $P_2$  are the partials, which have components  $\alpha_1$  and  $\alpha_2$  in edge orientation and  $\beta_1$  and  $\beta_2$  in screw orientation.  $r$  is the equilibrium separation of the partials, which will further separate under a stress  $\tau$ . Dashed lines indicate the new position of the partials.

<sup>\*</sup>3 indices notation will be used throughout hereafter.

Strength of  $\beta_1$  and  $\beta_2$  along  $[111]$  is given by,

$$\frac{\frac{a}{6} [111] [4\bar{1}\bar{2}]}{\sqrt{3}} = \frac{a}{2\sqrt{3}} \quad (3)$$

and that of  $\alpha_1$  and  $\alpha_2$  along the  $[10\bar{1}]$  direction is given by

$$\frac{a}{6} \cdot \frac{[2\bar{1}\bar{4}] [10\bar{1}]}{\sqrt{2}} = \frac{a}{\sqrt{2}} \quad (4)$$

$\beta_1$  and  $\beta_2$  attract each other and  $\alpha_1$  and  $\alpha_2$  repel each other which is obvious from the sense of their Burgers vectors.

Force of repulsion between the edge components  $\alpha_1$  and  $\alpha_2$  is given by,

$$R_1 = \frac{\mu a^2}{2\pi(1-\nu)r} = \frac{3\mu a^2}{8\pi r} \quad (5)$$

$\mu$  = shear modulus

$\nu$  = Poissons ratio = 1/3

and  $a = \alpha_1 = \alpha_2$

similarly, force of attraction between the screw components  $\beta_1$  and  $\beta_2$  is given by,

$$R_2 = \frac{\mu \beta^2}{2\pi r} = \frac{\mu a^2}{24\pi r} \quad (6)$$

Therefore, the net repulsive force

$$R_1 - R_2 = \frac{\mu a^2}{3\pi r} \quad (7)$$

Equation (7) can be written in terms of the Burgers vector of the complete dislocation, giving

$$R_1 - R_2 = \frac{\mu b^2}{6\pi r} \quad (8)$$

In equilibrium, the repulsive force of the partials is balanced by the attractive force of the stacking fault, hence

$$\gamma = \frac{\mu b^2}{6 \pi r} \quad (9)$$

where

$$\begin{aligned} \gamma &= \text{stacking fault energy in ergs/cm}^2 \\ r &= \text{separation of partials in cm.} \end{aligned}$$

In the presence of an internal stress  $\tau$ , equation (9) will be replaced by

$$\gamma = \frac{\mu b^2}{6 \pi r} + \tau \beta \quad (10)$$

Here,  $\tau$  will be assumed to be the internal stress anchoring the partials away from its equilibrium position. Let us assume that the anchoring stress is due to an identical dislocation lying in a parallel plane. If the dislocation density at 15 % cold work be assumed to be  $\sim 10^{12}/\text{cm}^2$ , the average distance between the dislocations will be about  $10^{-6}$  cm.

$$\begin{aligned} \text{Then } \tau &\approx \frac{\mu b}{2 \pi l} \\ &\approx 2 \sqrt{2} \times 10^9 \text{ dynes/cm}^2 \end{aligned} \quad (11)$$

$$\text{where } \mu \approx 4 \times 10^{11} \text{ dynes/cm}^2$$

$$\text{and } \tau \beta = \sqrt{42} \times 10 \text{ dynes/cm}^2 \quad (12)$$

Substituting (12) and the measured value of  $r$  in (10) gives,

$$\gamma - 65 \approx 0.2 \quad (13)$$

$$\text{or } \gamma \approx 65 \text{ ergs/cm}^2 \quad (14)$$

This value, however, can be in error by a factor of 2.

Substituting (14) in (9), the equilibrium separation of partials,

$$r \approx 62 \text{ \AA} \quad (15)$$

Under a magnification of 20,000, the equilibrium separation will be  $\approx 0.12$  mm. In most cases the fault plane will be inclined to the plane of projection and hence the separation will be even smaller.

Substituting (3) in (10) for  $\beta$ , and using the value  $\frac{\mu b^2}{6 \pi r} \approx 0.2$ ,

$$\gamma - \frac{\tau a}{2\sqrt{3}} \approx 0.2$$

or  $\tau \approx 19 \times 10^{-3} \mu \quad (16)$

From above it is clear that a normal stress in excess of  $19 \times 10^{-3} \mu$  acting in the  $(1\bar{1}00)$  plane is needed to separate the partials from their equilibrium position. It is quite a large stress and perhaps is the reason why stacking faults appear only at high deformations.

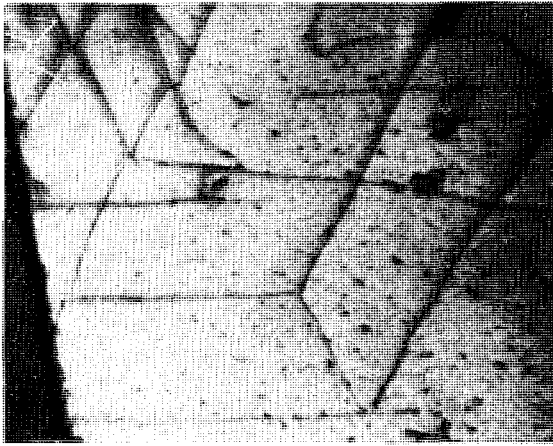


Fig. 1 a Straight dislocations in Zr  
40.000 x

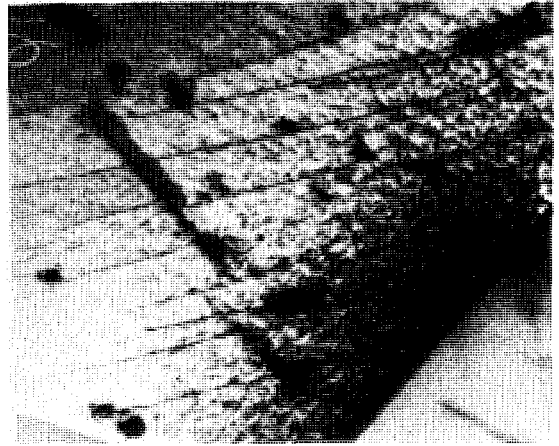


Fig. 1 b Straight dislocations in  
Zircaloy-2 40.000 x

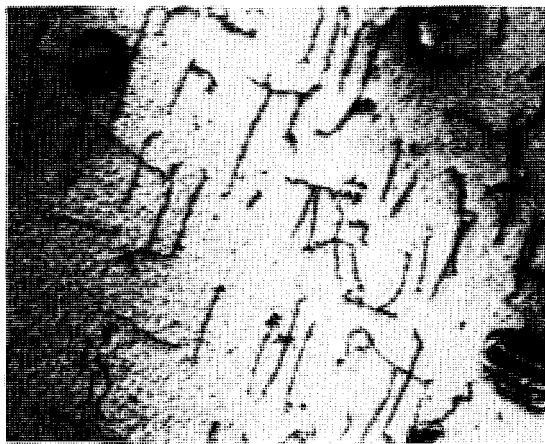


Fig. 2 a Short dislocations in Zr  
40.000 x

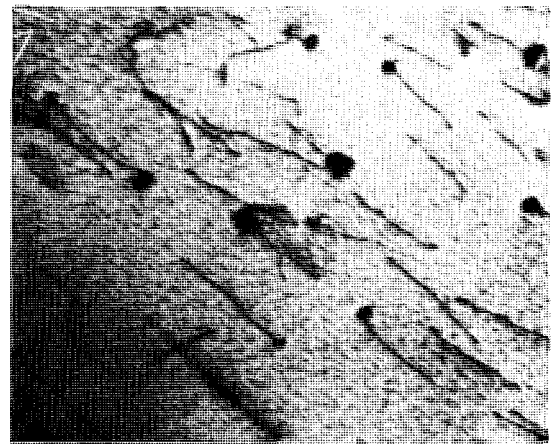


Fig. 2 b Short dislocations in  
Zircaloy-2 40.000 x

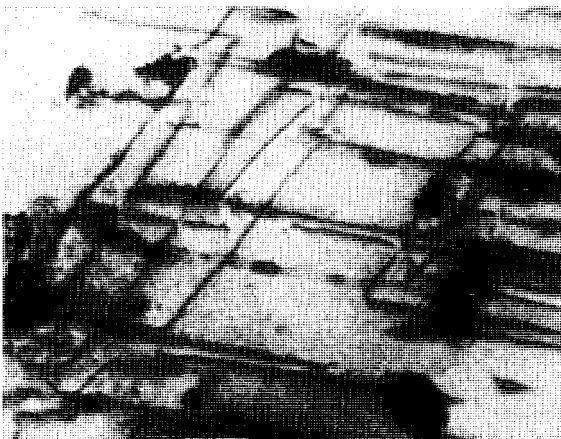


Fig. 3 a Intersecting pairs of  
dislocations in Zr  
40.000 x



Fig. 3 b Intersecting pairs of  
dislocations in Zircaloy-2  
40.000 x

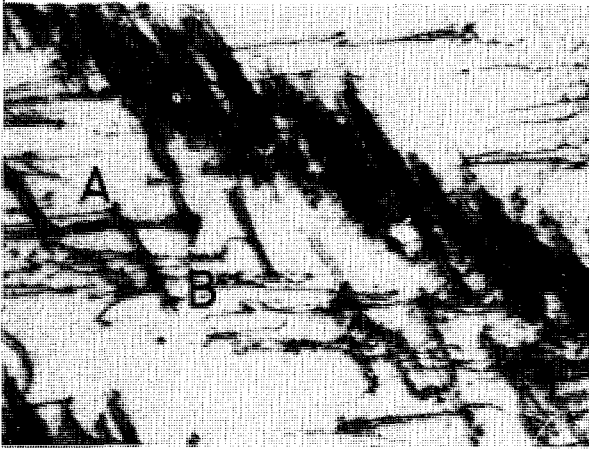


Fig. 4 a Band of paired dislocations  
(or dipoles)  
40.000 ×



Fig. 4 b Band of paired dislocations  
(or elongated loops) in  
Zircaloy-2 30.000 ×

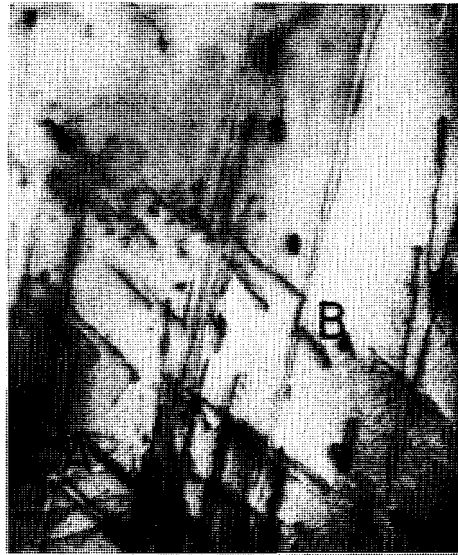


Fig. 5 Pairs of long dislocations interacting  
with dislocations in an intersecting  
plane. Wavy nature of the dislocations  
suggest they are screw. Notice  
interactions at A & B. Zircaloy-2

40.000 ×



Fig. 6 Interaction of a long sweeping dislocation with a family of short dislocation. Notice reactions at C, D, & E. Zircaloy-2 (10% CW)  
20.000 x



Fig. 7 Paired dislocations (or elongated loops) lying in  $(10\bar{1}0)$  planes, Zircaloy-2 (10% CW)  
30.000 x



Fig. 8 Dislocations lying in  $(10\bar{1}0)$  plane in 10% CW Zr  
20.000 x



Fig. 9 Dipoles and elongated loop in 10% cold worked Zr  
40.000 x



Fig. 10 Paired dislocations lying in  $(10\bar{1}0)$  and  $(01\bar{1}2)$  planes in 10% cold worked Zircaloy-2  
20,000 ×



Fig. 11 Short dislocations lying in  $(10\bar{1}0)$  planes in 10% C.W. Zircaloy-2. These dislocations are of mixed type and are predominantly edge in character.  
20,000 ×



Fig. 12 Note dislocation cusp at A and junction reactions below A. Zircaloy-2 (10% cold work)

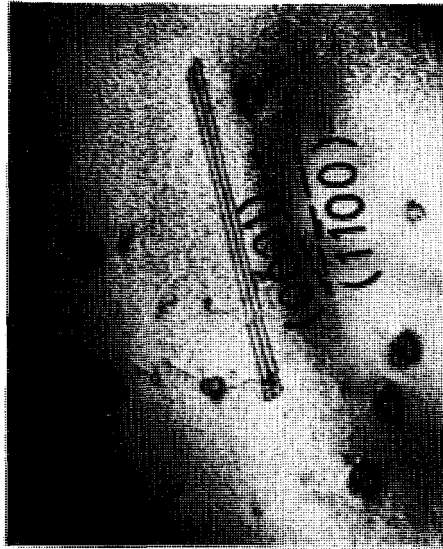


Fig. 13 Stacking fault ribbon lying  
in  $(10\bar{1}0)$  plane in 15 %  
cold rolled Zircaloy-2  
20.000  $\times$

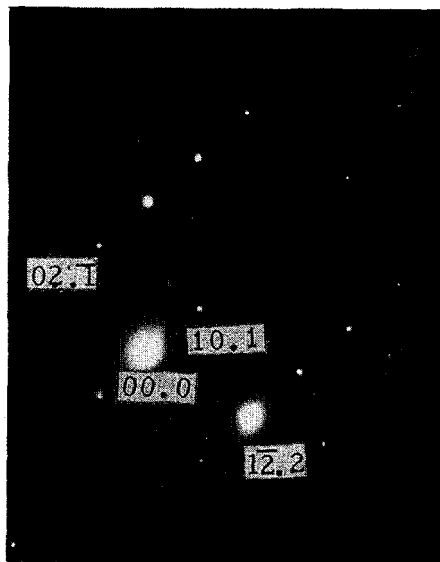


Fig. 14 Selected area diffraction  
pattern from an area near  
the stacking fault.

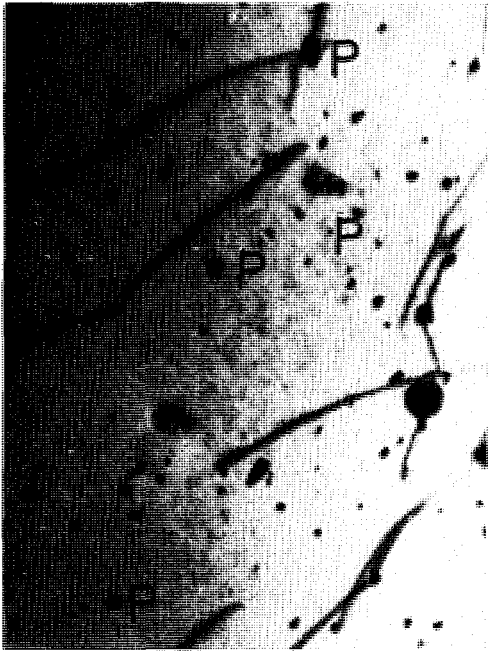


Fig. 15 Irradiation induced precipitation in Zr. Notice the pinned dislocations and precipitates at point P. These dislocations lie in  $(10\bar{1}0)$  plane.

20.000 ×

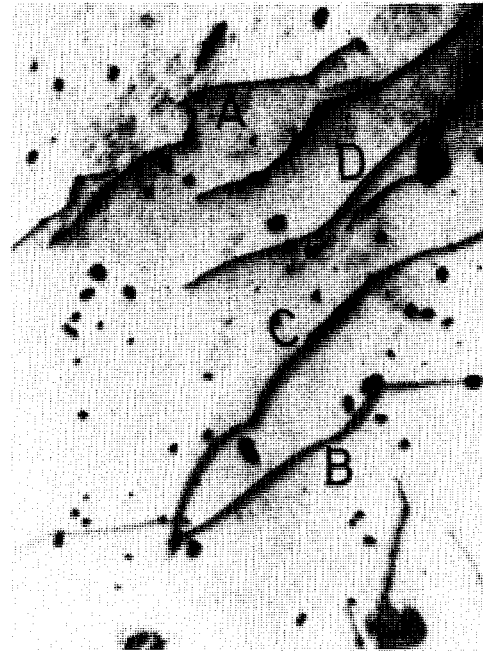


Fig. 16 Some more pinned dislocations in double contrast. But notice  
 i) at A, part of dislocation shows only single contrast  
 ii) at B, separation of image has narrowed down due to pinning  
 iii) Peculiar contrast at C.

20.000 ×

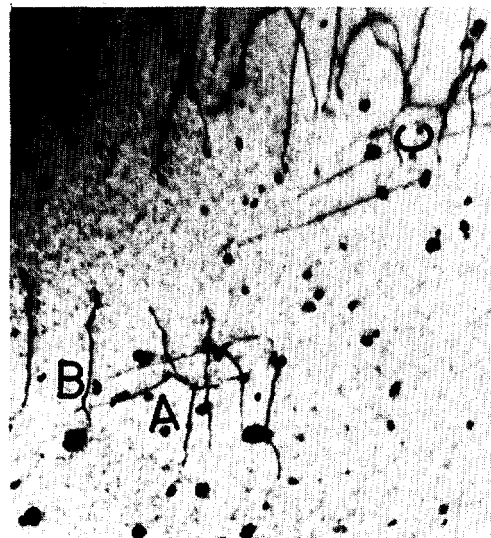


Fig. 17 Pinned dislocations and their tendency to form tangles. Note dislocation reaction products at A, B and C

20.000 ×



Fig. 18 Notice elongated loop contrast at A, B and C. (Irradiated Zr).

20.000 x



Fig. 19 Same as fig. 18 but the specimen was tilted. Notice that some of the loop contrasts have changed to line contrasts e.g. at B and D

20.000 x



Fig. 20 General loop contrasts of defects in irradiated Zr

20.000 x

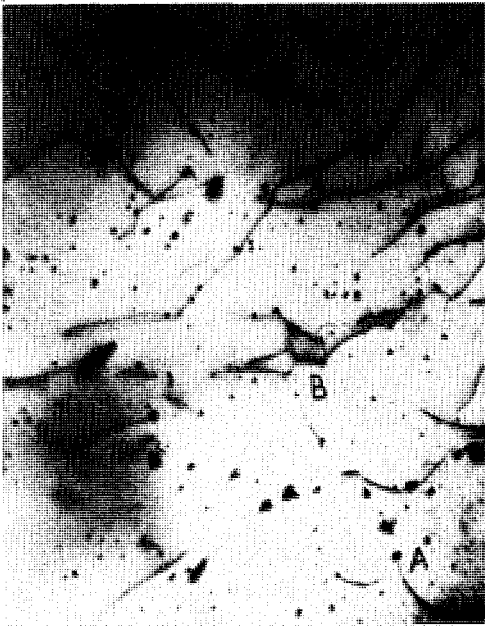


Fig. 21 Strong pinning action in irradiated Zr. Notice A and B.

20.000 x

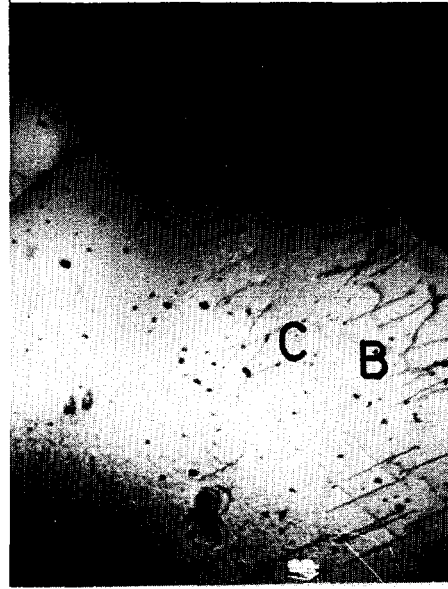


Fig. 22 Note pile-ups at A and cross-slip at C and tangling tendency at B

20.000 x



LIST OF PUBLISHED AE-REPORTS

1—50. (See the back cover earlier reports.)

51. Activation analysis of aluminium. By D. Brune. 1961. 8 p. Sw. cr. 6:—.
52. Thermo-technical data for D<sub>2</sub>O. By E. Axbom. 1961. 14 p. Sw. cr. 6:—.
53. Neutron damage in steels containing small amounts of boron. By H. P. Myers. 1961. 23 p. Sw. cr. 6:—.
54. A chemical eight group separation method for routine use in gamma spectrometric analysis. I. Ion exchange experiments. By K. Samsahl. 1961. 13 p. Sw. cr. 6:—.
55. The Swedish zero power reactor R0. By Olof Landergård, Kaj Cavallin and Georg Jonsson. 1961. 31 p. Sw. cr. 6:—.
56. A chemical eight group separation method for routine use in gamma spectrometric analysis. II. Detailed analytical schema. By K. Samsahl. 18 p. 1961. Sw. cr. 6:—.
57. Heterogeneous two-group diffusion theory for a finite cylindrical reactor. By Alf Jonsson and Göran Näslund. 1961. 20 p. Sw. cr. 6:—.
58. Q-values for (n, p) and (n,  $\alpha$ ) reactions. By J. Konijn. 1961. 29 p. Sw. cr. 6:—.
59. Studies of the effective total and resonance absorption cross section for zircaloy 2 and zirconium. By E. Hellstrand, G. Lindahl and G. Lundgren. 1961. 26 p. Sw. cr. 6:—.
60. Determination of elements in normal and leukemic human whole blood by neutron activation analysis. By D. Brune, B. Frykberg, K. Samsahl and P. O. Wester. 1961. 16 p. Sw. cr. 6:—.
61. Comparative and absolute measurements of 11 inorganic constituents of 38 human tooth samples with gamma-ray spectrometry. By K. Samsahl and R. Söremark. 19 p. 1961. Sw. cr. 6:—.
62. A Monte Carlo sampling technique for multi-phonon processes. By Thure Högberg. 10 p. 1961. Sw. cr. 6:—.
63. Numerical integration of the transport equation for infinite homogeneous media. By Rune Håkansson. 1962. 15 p. Sw. cr. 6:—.
64. Modified Suessmuth balances for ferromagnetic and paramagnetic measurements. By N. Lundquist and H. P. Myers. 1962. 9 p. Sw. cr. 6:—.
65. Irradiation effects in strain aged pressure vessel steel. By M. Grounes and H. P. Myers. 1962. 8 p. Sw. cr. 6:—.
66. Critical and exponential experiments on 19-rod clusters (R3-fuel) in heavy water. By R. Persson, C-E. Wikdahl and Z. Zadworski. 1962. 34 p. Sw. cr. 6:—.
67. On the calibration and accuracy of the Guinier camera for the determination of interplanar spacings. By M. Möller. 1962. 21 p. Sw. cr. 6:—.
68. Quantitative determination of pole figures with a texture goniometer by the reflection method. By M. Möller. 1962. 16 p. Sw. cr. 6:—.
69. An experimental study of pressure gradients for flow of boiling water in a vertical round duct, Part I. By K. M. Becker, G. Hernborg and M. Bode. 1962. 46 p. Sw. cr. 6:—.
70. An experimental study of pressure gradients for flow of boiling water in a vertical round duct, Part II. By K. M. Becker, G. Hernborg and M. Bode. 1962. 32 p. Sw. cr. 6:—.
71. The space-, time- and energy-distribution of neutrons from a pulsed plane source. By A. Claesson. 1962. 16 p. Sw. cr. 6:—.
72. One-group perturbation theory applied to substitution measurements with void. By R. Persson. 1962. 21 p. Sw. cr. 6:—.
73. Conversion factors. By A. Amberntson and S-E. Larsson. 1962. 15 p. Sw. cr. 10:—.
74. Burnout conditions for flow of boiling water in vertical rod clusters. By Kurt M. Becker. 1962. 44 p. Sw. cr. 6:—.
75. Two-group current-equivalent parameters for control rod cells. Autocode programme CRCC. By O. Norinder and K. Nyman. 1962. 18 p. Sw. cr. 6:—.
76. On the electronic structure of MnB. By N. Lundquist. 1962. 16 p. Sw. cr. 6:—.
77. The resonance absorption of uranium metal and oxide. By E. Hellstrand and G. Lundgren. 1962. 17 p. Sw. cr. 6:—.
78. Half-life measurements of <sup>6</sup>He, <sup>16</sup>N, <sup>19</sup>O, <sup>20</sup>F, <sup>24</sup>Al, <sup>77</sup>Se<sup>m</sup> and <sup>110</sup>Ag. By J. Konijn and S. Malmkog. 1962. 34 p. Sw. cr. 6:—.
79. Progress report for period ending December 1961. Department for Reactor Physics. 1962. 53 p. Sw. cr. 6:—.
80. Investigation of the 800 keV peak in the gamma spectrum of Swedish Laplanders. By I. O. Andersson, I. Nilsson and K. Eckerstig. 1962. 8 p. Sw. cr. 6:—.
81. The resonance integral of niobium. By E. Hellstrand and G. Lundgren. 1962. 14 p. Sw. cr. 6:—.
82. Some chemical group separations of radioactive trace elements. By K. Samsahl. 1962. 18 p. Sw. cr. 6:—.
83. Void measurement by the ( $\gamma$ , n) reactions. By S. Z. Rouhani. 1962. 17 p. Sw. cr. 6:—.
84. Investigation of the pulse height distribution of boron trifluoride proportional counters. By I. O. Andersson and S. Malmkog. 1962. 16 p. Sw. cr. 6:—.
85. An experimental study of pressure gradients for flow of boiling water in vertical round ducts. (Part 3). By K. M. Becker, G. Hernborg and M. Bode. 1962. 29 p. Sw. cr. 6:—.
86. An experimental study of pressure gradients for flow of boiling water in vertical round ducts. (Part 4). By K. M. Becker, G. Hernborg and M. Bode. 1962. 19 p. Sw. cr. 6:—.
87. Measurements of burnout conditions for flow of boiling water in vertical round ducts. By K. M. Becker. 1962. 38 p. Sw. cr. 6:—.
88. Cross sections for neutron inelastic scattering and (n, 2n) processes. By M. Leimdörfer, E. Bock and L. Arkeryd. 1962. 225 p. Sw. cr. 10:—.
89. On the solution of the neutron transport equation. By S. Depken. 1962. 43 p. Sw. cr. 6:—.
90. Swedish studies on irradiation effects in structural materials. By M. Grounes and H. P. Myers. 1962. 11 p. Sw. cr. 6:—.
91. The energy variation of the sensitivity of a polyethylene moderated BF<sub>3</sub> proportional counter. By R. Fräki, M. Leimdörfer and S. Malmkog. 1962. 12. Sw. cr. 6:—.
92. The backscattering of gamma radiation from plane concrete walls. By M. Leimdörfer. 1962. 20 p. Sw. cr. 6:—.
93. The backscattering of gamma radiation from spherical concrete walls. By M. Leimdörfer. 1962. 16 p. Sw. cr. 6:—.
94. Multiple scattering of gamma radiation in a spherical concrete wall room. By M. Leimdörfer. 1962. 18 p. Sw. cr. 6:—.
95. The paramagnetism of Mn dissolved in  $\alpha$  and  $\beta$  brasses. By H. P. Myers and R. Westin. 1962. 13 p. Sw. cr. 6:—.
96. Isomorphic substitutions of calcium by strontium in calcium hydroxyapatite. By H. Christensen. 1962. 9 p. Sw. cr. 6:—.
97. A fast time-to-pulse height converter. By O. Aspelund. 1962. 21 p. Sw. cr. 6:—.
98. Neutron streaming in D<sub>2</sub>O pipes. By J. Braun and K. Randén. 1962. 41 p. Sw. cr. 6:—.
99. The effective resonance integral of thorium oxide rods. By J. Weitman. 1962. 41 p. Sw. cr. 6:—.
100. Measurements of burnout conditions for flow of boiling water in vertical annuli. By K. M. Becker and G. Hernborg. 1962. 41 p. Sw. cr. 6:—.
101. Solid angle computations for a circular radiator and a circular detector. By J. Konijn and B. Tollander. 1963. 6 p. Sw. cr. 8:—.
102. A selective neutron detector in the keV region utilizing the <sup>19</sup>F(n,  $\gamma$ )<sup>20</sup>F reaction. By J. Konijn. 1963. 21 p. Sw. cr. 8:—.
103. Anion-exchange studies of radioactive trace elements in sulphuric acid solutions. By K. Samsahl. 1963. 12 p. Sw. cr. 8:—.
104. Problems in pressure vessel design and manufacture. By O. Hellström and R. Nilson. 1963. 44 p. Sw. cr. 8:—.
105. Flame photometric determination of lithium contents down to 10<sup>-3</sup> ppm in water samples. By G. Jönsson. 1963. 9 p. Sw. cr. 8:—.
106. Measurements of void fractions for flow of boiling heavy water in a vertical round duct. By S. Z. Rouhani and K. M. Becker. 1963. 2nd rev. ed. 32 p. Sw. cr. 8:—.
107. Measurements of convective heat transfer from a horizontal cylinder rotating in a pool of water. K. M. Becker. 1963. 20 p. Sw. cr. 8:—.
108. Two-group analysis of xenon stability in slab geometry by modal expansion. O. Norinder. 1963. 50 p. Sw. cr. 8:—.
109. The properties of CaSO<sub>4</sub>Mn thermoluminescence dosimeters. B. Bjärngård. 1963. 27 p. Sw. cr. 8:—.
110. Semianalytical and seminumerical calculations of optimum material distributions. By C. I. G. Andersson. 1963. 26 p. Sw. cr. 8:—.
111. The paramagnetism of small amounts of Mn dissolved in Cu-Al and Cu-Ge alloys. By H. P. Myers and R. Westin. 1963. 7 p. Sw. cr. 8:—.
112. Determination of the absolute disintegration rate of Cs<sup>137</sup>-sources by the tracer method. S. Hellström and D. Brune. 1963. 17 p. Sw. cr. 8:—.
113. An analysis of burnout conditions for flow of boiling water in vertical round ducts. By K. M. Becker and P. Persson. 1963. 28 p. Sw. cr. 8:—.
114. Measurements of burnout conditions for flow of boiling water in vertical round ducts (Part 2). By K. M. Becker, et al. 1963. 29 p. Sw. cr. 8:—.
115. Cross section measurements of the <sup>58</sup>Ni(n, p)<sup>58</sup>Co and <sup>29</sup>Si(n,  $\alpha$ )<sup>26</sup>Mg reactions in the energy range 2.2 to 3.8 MeV. By J. Konijn and A. Lauber. 1963. 30 p. Sw. cr. 8:—.
116. Calculations of total and differential solid angles for a proton recoil solid state detector. By J. Konijn, A. Lauber and B. Tollander. 1963. 31 p. Sw. cr. 8:—.
117. Neutron cross sections for aluminium. By L. Forsberg. 1963. 32 p. Sw. cr. 8:—.
118. Measurements of small exposures of gamma radiation with CaSO<sub>4</sub>Mn radiothermoluminescence. By B. Bjärngård. 1963. 18 p. Sw. cr. 8:—.
119. Measurement of gamma radioactivity in a group of control subjects from the Stockholm area during 1959—1963. By I. O. Andersson, I. Nilsson and Eckerstig. 1963. 19 p. Sw. cr. 8:—.
120. The thermox process. By O. Tjälldin. 1963. 38 p. Sw. cr. 8:—.
121. The transistor as low level switch. By A. Lydén. 1963. 47 p. Sw. cr. 8:—.
122. The planning of a small pilot plant for development work on aqueous reprocessing of nuclear fuels. By T. U. Sjöborg, E. Haefner and Hultgren. 1963. 20 p. Sw. cr. 8:—.
123. The neutron spectrum in a uranium tube. By E. Johansson, E. Jonsson, M. Lindberg and J. Mednis. 1963. 36 p. Sw. cr. 8:—.
124. Simultaneous determination of 30 trace elements in cancerous and non-cancerous human tissue samples with gamma-ray spectrometry. K. Samsahl, D. Brune and P. O. Wester. 1963. 23 p. Sw. cr. 8:—.
125. Measurement of the slowing-down and thermalization time of neutrons in water. By E. Möller and N. G. Sjöstrand. 1963. 42 p. Sw. cr. 8:—.
126. Report on the personnel dosimetry at AB Atomenergi during 1962. By K-A. Edvardsson and S. Hagsgård. 1963. 12 p. Sw. cr. 8:—.
127. A gas target with a tritium gas handling system. By B. Holmqvist and T. Wiedling. 1963. 12 p. Sw. cr. 8:—.
128. Optimization in activation analysis by means of epithermal Neutrons. Determination of molybdenum in steel. By D. Brune and K. Jirlow. 1963.
129. The P<sub>1</sub>-approximation for the distribution of neutrons from  $\alpha$  pulsed source in hydrogen. By A. Claesson. 1963.
130. Dislocation arrangements in deformed and neutron irradiated zirconium and zircaloy-2. By R. B. Roy. 1963. Sw. cr. 8:—.

Förteckning över publicerade AES-rapporter

1. Analys medelst gamma-spektrometri. Av D. Brune. 1961. 10 s. Kr 6:—.
  2. Bestrålningsförändringar och neutronatmosfär i reaktortrycktankar — några synpunkter. Av M. Grounes. 1962. 33 s. Kr 6:—.
  3. Studium av sträckgränsen i mjukt stål. G. Östberg, R. Athermo. 1963. 17 s. Kr 6:—.
  4. Teknisk utvärdering inom reaktorområdet. Erik Jonson. 1963. 64 s. Kr. 8:—.
- Additional copies available at the library of AB Atomenergi, Studsvik, Nyköping, Sweden. Transport microcards of the reports are obtainable through the International Documentation Center, Tumba, Sweden.